行政院國家科學委員會補助專題研究計畫 □成果報告 ■期中進度報告

以電鍍法製作含奈米粒子之金屬微結構的熱膨脹係數及疲勞特性研究(1/3)

計畫類別：■ 個別型計畫　□ 整合型計畫
計畫編號：NSC 97 － 2221 － E － 009 － 020 － MY3
執行期間： 97 年 08 月 01 日至 100 年 07 月 31 日

計畫主持人：徐文祥
共同主持人：
計畫參與人員：黃家聖，蔡梨暖，李毅家，林軒宇

成果報告類型(依經費核定清單規定繳交)：■精簡報告 □完整報告

本成果報告包括以下應繳交之附件：
□赴國外出差或研習心得報告一份
□赴大陸地區出差或研習心得報告一份
■出席國際學術會議心得報告及發表之論文各一份
□國際合作研究計畫國外研究報告書一份

處理方式：除產學合作研究計畫、提升產業技術及人才培育研究計畫、列管計畫及下列情形者外，得立即公開查詢
□涉及專利或其他智慧財產權，□一年□二年後可公開查詢

執行單位：國立交通大學機械系

中 華 民 國 98 年 05 月 14 日

中文摘要：

本研究利用低溫電鍍鎳製程技術，個別於鍍液中加入不同粒徑尺寸的奈米鑽石顆粒(350nm, 125nm, 和 50nm)和二氧化矽顆粒(80nm)，共同沈積形成電鍍鎳基複合材料，以討論“奈米複材效應”於材料熱膨脹係數與楊氏係數的變化。由實驗結果得知，藉由不同粒子的添加，可以調控複合材料熱膨脹係數與楊氏係數的提升或衰減。本實驗室是首先發現金屬奈米複材有提升熱膨脹係數特性的研究團隊，雖然複合材料楊氏係數的強化，可以藉由傳統混合法則解釋；但是對於熱膨脹係數的強化，卻無法以通常的混合法則解釋之。於本研究中，從 X 光繞射圖譜(XRD)的觀察，獲得複合材料中殘留應力形態與複合材料熱膨脹係數間的關係；並由穿透式電子顯微鏡(TEM)觀察奈米顆粒鑲嵌於基材中的位置，成功地解釋複合材料的殘留應力形態變化與其熱膨脹係數間的關係。

關鍵詞：奈米複材，電鍍，鎳，奈米鑽石粒子，熱膨脹係數

英文摘要：

Employing a low-temperature electroplated Ni process with the addition of uniformly dispersed nano-particles of diamond (average diameter 350nm, 125nm, and 50nm) and SiO_2 (average diameter 80 nm), “nanocomposite effects” are investigated for the modification of thermal expansion coefficient (CTE) and Young’s modulus. Experimental results show that these material parameters can be either enhanced or deteriorated via the incorporation of different kind of nano-particles. Although the enhancement of mechanical strength can be attributed to the intrinsic characteristics of nano-particle based on the rule of mixture, the discrepancy of CTE modification can only be explained by X-ray diffraction (XRD) and transmission electron microscope (TEM) analysis on residual stress type resulting in the CTE variation.

Key words： Nanocomposite, Electroplating, Ni, nano diamond particle, CTE,

報告內容：

1. Introduction

Electro-deposition has been a manifest process technique for cost-effective MEMS (microelectromechanical systems) fabrication. This technique provides several advantages including flexible material choice, low temperature CMOS compatible process, and high manufacturing throughput. For instance, electroplated Ni can have comparable mechanical properties with poly-silicon but even lower electrical and thermal resistivity, lower processing temperature, and higher deposition rate. Since 1988, lots of research works have been done in the electroplated Ni for MEMS fabrication and application [1-6].

Recently, the nanotechnology has further advanced the electroplating technique in terms of material property enhancement for various MEMS applications. Combining with the strengthening and size effects originated from the incorporation of well distributed nano-particles like diamond, SiC, Al_2O_3, and Si_3N_4 [7-12], electroplated metal-nanocomposite can exhibit superior physical properties beyond the limits of intrinsic metal. Teh *et al.* [10] have shown Ni-based nanocomposite synthesis method for MEMS devices fabrication. Huang *et al.* [11] have demonstrated a low power magnetic microactuator using Cu-Ni nanocomposite as the inductive coil material. For electro-thermal microactuator application, Tsai *et al.* [12] have shown that the microactuator made of Ni-diamond nanocomposite can reduce 73% power requirement of pure Ni one needed for the same output displacement of 3 μm and enlarge the reversible displacement range from 1.8 to 3 μm, simultaneously. The performance enhancements are resulted by the augment of coefficient of thermal expansion (CTE) and hardness of Ni via the nano-diamond particle incorporation. Thus, employing the nanocomposites synthesized by electro-deposition process for MEMS fabrication has revealed its excellent prospect.

This presented work will investigate nano-particle size and composite effects on the modification of material properties of electroplated Ni. Via the understanding of the correlation, such a Ni-based nanocomposite provides an alternative research direction in the future development of MEMS fabrication using nanocomposites.

2. Fabrication

In the prior work [12], cantilever beams made of electroplated Ni or Ni-diamond nanocomposite were utilized for characterizing the CTE property. By measuring the elongation of cantilever beam in a heated chamber with temperature control, the CTE of material can be obtained. The cantilevers are all fabricated using the electroplating Ni process with the addition of uniformly dispersed nano-particles. Different sizes of nano-diamond particles, which are 350 nm, 125 nm, and 50 nm in average diameter respectively, will be added into a sulfuric based Ni plating bath for the investigation of size effect and 80 nm in average diameter of nano-SiO_2 particle is chosen here for comparison purpose, which will be discussed later. The amount of nano-particle incorporation in Ni matrix is controlled using different plating bath with different particle concentration. In the experiment, the Ni-diamond and Ni-SiO_2 nanocomposites are synthesized in different plating

solutions, which have the concentration of the nano-diamond particles ranging from 0 to 2 g/L and the concentration of the nano-SiO_2 particles ranging from 0 to 0.036 g/L, respectively. Table 1 shows the detail plating bath compositions, conditions, and the concentration of nano-particles in the bath.

Table 1. Plating bath conditions of Ni-diamond and Ni-SiO_2 nanocomposite.

Ni-diamond nanocomposite	
Batch:	
Nickel sulfamate (g/L)	400
Nickel chloride (g/L)	5
Boric acid (g/L)	40
Wetting agent (c.c.)	5
Concentration of diamond nano-particle (g/L)	2, 1, 0.5
Average diameter of diamond nano-particle (nm)	350, 125, 50
pH	4.1 ~ 4.3
Current density (mA/cm^2)	10
Temperature (°C)	50
Ni-SiO_2 nanocomposite	
Batch:	
Nickel sulfamate (g/L)	400
Nickel chloride (g/L)	5
Boric acid (g/L)	40
Wetting agent (c.c.)	5
Concentration of SiO_2 nano-particle (g/L)	0.008, 0.018, 0.036
Average diameter of SiO_2 nano-particle (nm)	80
pH	4.1 ~ 4.3
Current density (mA/cm^2)	10
Temperature (°C)	50

As shown in Fig. 1, all device fabrication starts with a silicon wafer with 0.5 μm thick SiO_2 deposition followed by 2 μm thick FH-6400 photoresist (PR) coating. The PR is then patterned and hard baked as sacrificial layer. Then, a layer of 1000 Å Cu/100 Å Ti is sputtered as plating seed layer followed by another 8 μm thick AZP-4620 PR coating that is patterned as an electroplating mold. After that, Ni or Ni-based nanocomposite films are electroplated at 50 °C to form the cantilever beams. Finally, the fabricated cantilever beams are released after stripping the sacrificial layer by acetone solution. Fig. 2 shows the SEM micrographs of as-fabricated cantilever beams made of Ni-diamond and Ni-SiO_2 nanocomposites, respectively.

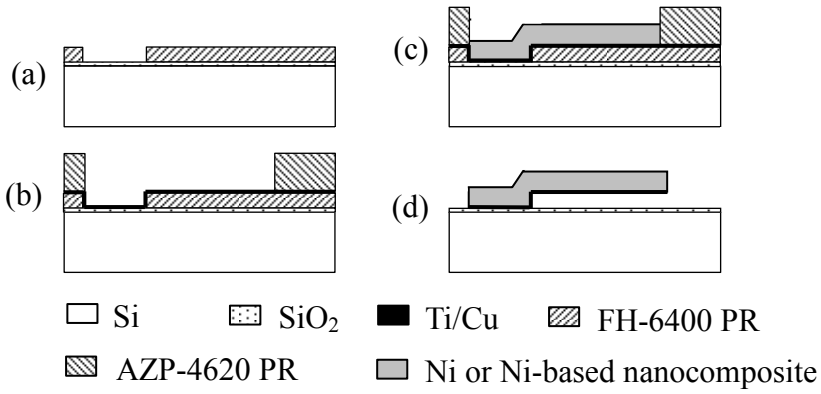

Fig. 1. Fabrication process of Ni-based cantilever beam.

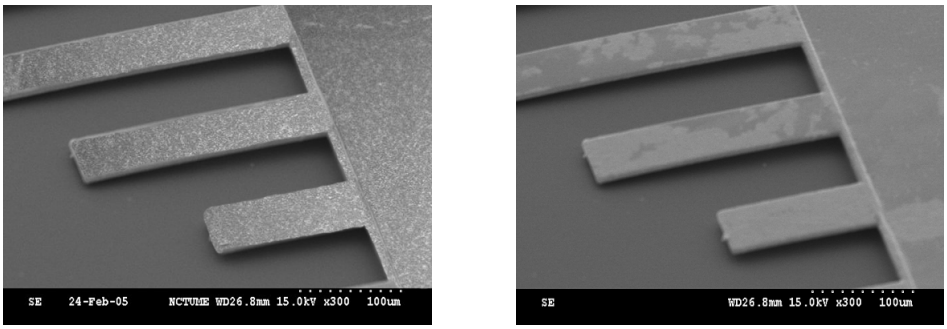

(a) **(b)**

Fig. 2. SEM pictures of fabricated cantilever beams made of: (a) Ni-diamond (average diameter 50 nm, 2 g/L), and (b) Ni-SiO_2 (average diameter 80 nm, 0.036 g/L) nanocomposites.

3. Results

3.1 Process characterizations

The plating process is characterized via the analysis of elemental analyzer (EA). The weight fractions of nano-diamonds in the Ni matrix with different plating concentrations are measured by EA as shown in Fig. 3. The volume fractions of nano-diamonds in the matrixes are calculated based on the density of nickel (8.908 g/cm^3) and the density of diamond powder (3.51 g/cm^3). The analyses show that the concentrations of the embedded nano-diamonds increase with the amount of the diamond powders being added into the plating bath. Besides, the smaller the nano-diamonds are put into the plating bath, the larger the volume fraction of the nano-diamonds will be incorporated in the Ni matrix. In contrast, because the EA cannot be used for the analysis of incorporated SiO_2 concentration in the Ni-SiO_2 nanocomposite system, the energy dispersive spectrum (EDS) is then used to examine the existence of SiO_2. Fig. 4 shows the spectrums of two samples which are pure Ni and the Ni-SiO_2 nanocomposite plated in the bath with the concentration of 0.036 g/L SiO_2. As compared, the nanocomposite has not only O peak but also Si peak with higher intensity than the pure Ni does, which could be attributed to the existence of incorporated SiO_2. Because there is no obvious spectrum difference between the pure Ni and the nanocomposites plated in the baths with 0.008 and 0.018 g/L SiO_2, respectively, it is suggested that the concentrations of the embedded nano-SiO_2 particles also increase with the amount of the

diamond powders being added into the plating bath.

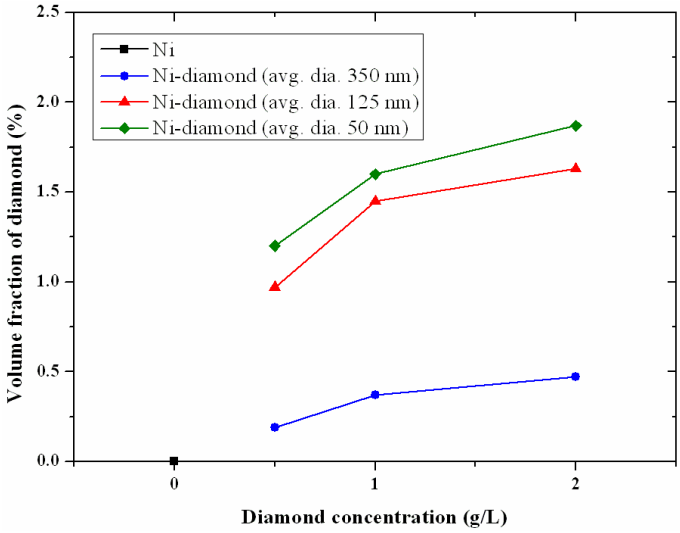

Fig. 3. Volume fractions of nano-diamonds in the Ni matrixes of different concentrations and average diameters of nano-diamond particles.

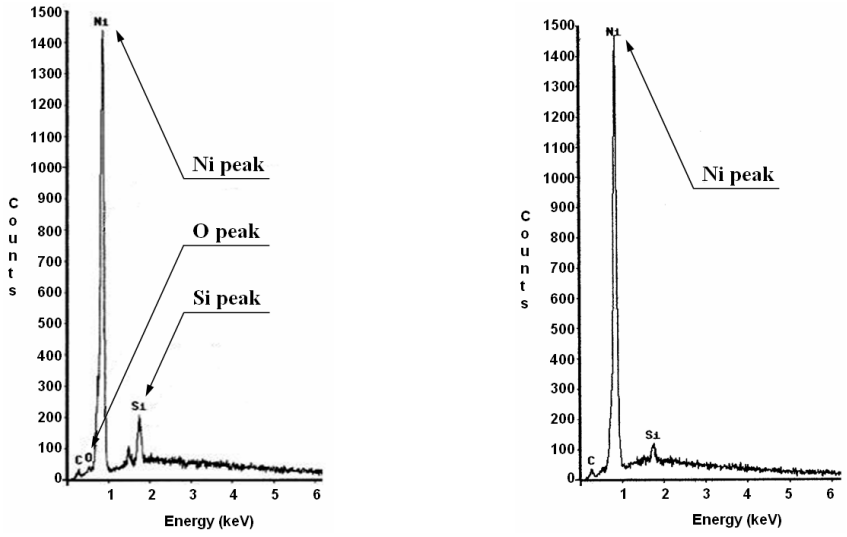

(a) **(b)**

Fig. 4**.** EDS spectrums of (a) Ni-SiO_2 nanocomposite (0.036 g/L) and (b) pure electroplated nickel.

3.2 CTE and Young's modulus characterizations

In the experiment, material CTE properties are investigated by measuring the elongation of cantilever beams made of electroplated Ni or Ni-based nanocomposite in a heating chamber at 400 °C. Fig. 5 compares the CTE properties of pure electroplated Ni and Ni-diamond nanocomposites with different concentrations and sizes of incorporated particles. Experiment results show that the CTE of Ni-diamond nanocomposites is higher than that of pure electroplated Ni (23 $\times 10^{-6}$/°C as measured) and increases with the concentration of incorporated nano-diamond. For the nanocomposites plated in a bath with 125 nm nano-diamonds, the CTE values increase from the

34.5 $\times 10^{-6}$/°C to 40.2 $\times 10^{-6}$/°C while the nano-diamond concentration in the bath increase from 1 to 2 g/L. Furthermore, more than two times enlargement of CTE value of Ni-diamond nanocomposite in average diameter 350 nm with the concentration of 2 g/L than pure electroplated Ni. However, with the reduction of the particle size of nano-diamond, the CTE values are found to decrease from 50 $\times 10^{-6}$/°C of the composite synthesized with the nano-diamonds of average diameter 350 nm down to 38 $\times 10^{-6}$/°C of that with the nano-diamonds of average diameter 50 nm. In contrast to nano-diamond particle, the CTE value decreases with the concentration of SiO_2 nano-particles in the plating bath from 22 $\times 10^{-6}$/°C of 0.008 g/L to 18 $\times 10^{-6}$/°C of 0.036 g/L.

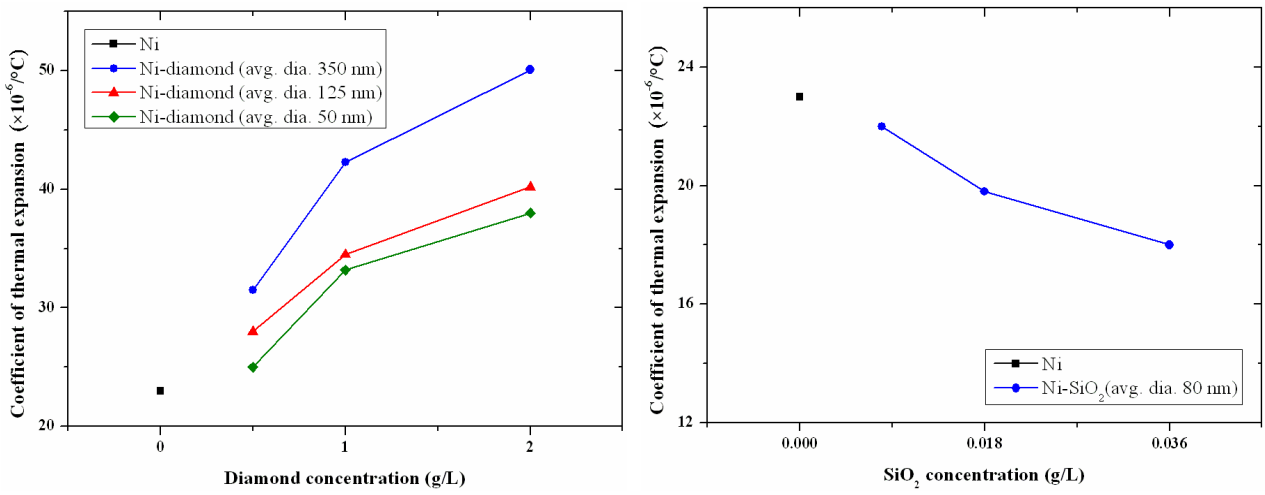

(a) (b)

Fig. 5. Comparison of CTE properties (at 400 °C) between pure electroplated Ni and Ni-based nanocomposites: (a) Ni-diamond and (b) Ni-SiO_2 with different particle sizes and concentrations.

In this work, Young's modulus is measured by means of a nanoindentation test using a Nano Indentor® XP from MTS Systems Corporation. Fig. 6 compares the Young's modulus of pure electroplated Ni and Ni-based nanocomposites, respectively, with different particle sizes and concentrations. The Young's modulus of Ni-diamond nanocomposites increases with the increase of diamond concentration and the decrease of nano-particle size. For a Ni-diamond nanocomposite plated with nano-diamond concentration of 2 g/L and particle size of 50 nm, the Young's modulus (~236.7 GPa, as measured) can be enhanced up to 1.24 times larger than that of pure electroplated Ni (~190.6 GPa, as measured). Because diamond has a higher Young's modulus (~1100 GPa [13]) than that of pure electroplated Ni, it can be expected that the material of Ni-diamond nanocomposite will have a higher Young's modulus, based on the rules of mixture [14]. It also explains that the modulus of Ni-SiO_2 nanocomposite decreases with the increase of SiO_2 concentration due to the lower Young's modulus of SiO_2 particle (~70 GPa [15]) relative to pure electroplated Ni. Being with the SiO_2 particle concentration of 0.036 g/L, the Young's modulus of the Ni-SiO_2 nanocomposite has been lowered down to 180 GPa.

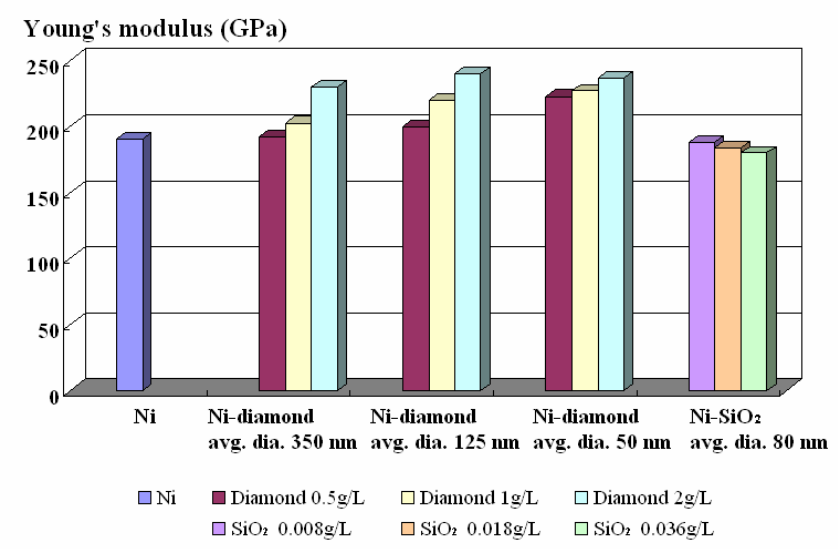

Fig. 6. Comparison of Young's modulus between pure electroplated Ni and Ni-based nanocomposites including Ni-diamond and Ni-SiO_2 with different particle sizes and concentrations.

3.3 Nanocomposite effects

As mentioned, although the incorporation of diamond particles in Ni matrix can augment CTE and Young's modulus parameters, the simple rule of mixture used for explaining conventional composite material's behavior [16-18] could not well qualitatively and quantitatively explain the discrepancy between the model prediction and the measurement results.

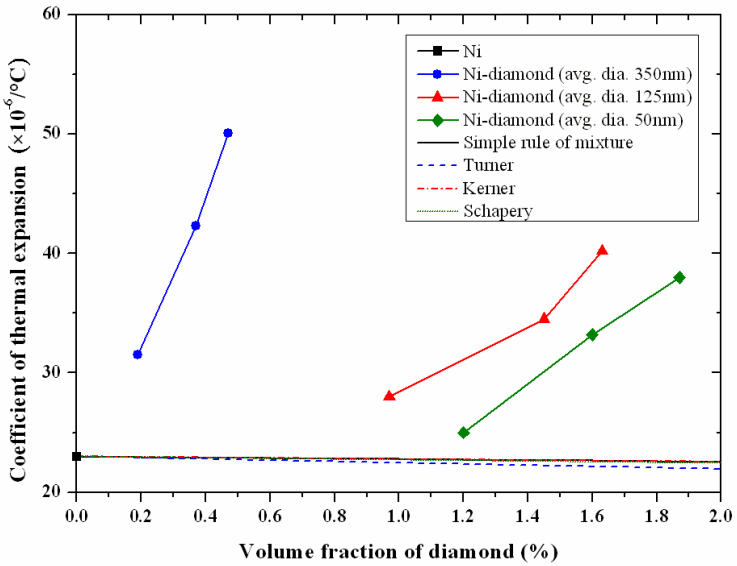

Fig. 7. Comparison of CTE between experimental data and model predictions of Ni-diamond nanocomposites.

Fig. 7, for instance, shows the CTE of Ni and Ni-diamond nanocomposites with For the CTE value of Ni-diamond nanocomposite (22.9 $\times 10^{-6}$/°C) from [16, 17]:

$$\alpha_c = V_m \alpha_m + V_p \alpha_p \qquad (1)$$

where α_c, α_m and α_p are CTEs of the composite, matrix (α_{Ni}: 23 $\times 10^{-6}$/°C, as measured) and particle ($\alpha_{diamond}$: 0.9 $\times 10^{-6}$/°C [19]), respectively. V_p is the volume fraction of the particle — an approximated 0.47% of nano-diamond particles occupied the Ni matrix. Although the CTE property of Ni-diamond nanocomposite doesn't conform to the simple rule of mixture, this discrepancy can be explained and further investigated by X-ray diffraction (XRD) analysis and transmission electron microscope (TEM) of the crystalline texture variation which result by the incorporation of nano-diamond particles. The correlation between nano-diamond particle effect and CTE property is demonstrated for electroplated Ni-diamond nanocomposite from XRD and TEM analysis.

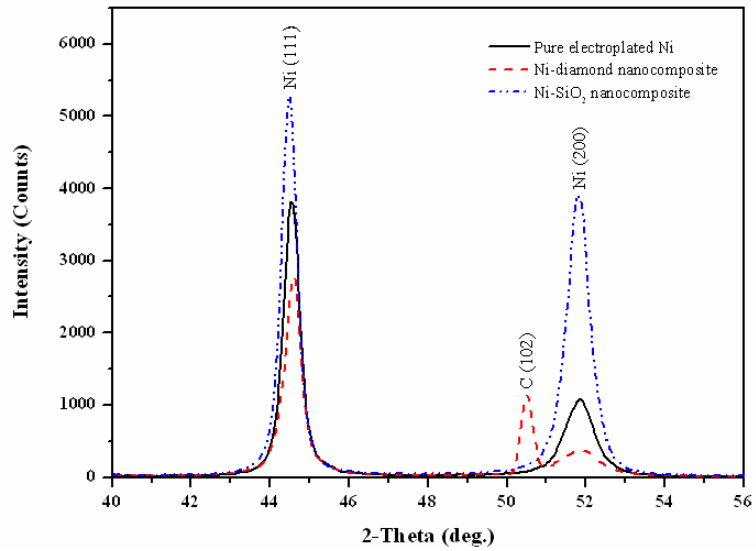

Fig. 8. The XRD patterns at room temperature for the as-fabricated pure Ni, Ni-diamond, and Ni-SiO_2 nanocomposites.

Fig. 8 shows the XRD patterns at room temperature for the as-fabricated pure Ni and Ni-based nanocomposites, respectively. The face-centered-cubic (FCC) texture of electroplated pure Ni and Ni-based nanocomposites have been observed with (111) preferred orientation of grain structure. From the comparison of peak-position between electroplated pure Ni and Ni-based nanocomposite, the residual stress types of Ni-diamond and Ni-SiO_2 nanocomposites can be determined easily by the variation of the lattice spacing as the following equation [20]:

$$\varepsilon = \frac{d' - d_0}{d_0} \qquad (2)$$

where d_0 is the lattice spacing of stress-free material, and d' is that for strained material. If we assume that pure electroplated Ni is stress-free material, and Ni-diamond and Ni-SiO_2 nanocomposites are strained materials. The strains of Ni-diamond and Ni-SiO_2 nanocomposites can be determined as -0.15% and 0.09%, respectively, from Eq. (2). Meanwhile, it can be obtained that the incorporation of nano-diamond particles in Ni causes compressive strain in nanocomposite, and the incorporation of SiO_2 nano-particles in Ni causes tensile strain in nanocomposite. Thus, residual compressive stress type is observed in Ni-diamond nanocomposite

with CTE enhancement. Oppositely, residual tensile stress type is observed in Ni-SiO_2 nanocomposite with CTE diminution. This result can also be found from the past research [21]. To further investigate the residual stress types resulted by the co-deposition of nano-particles with Ni, TEM analysis of crystalline texture is performed.

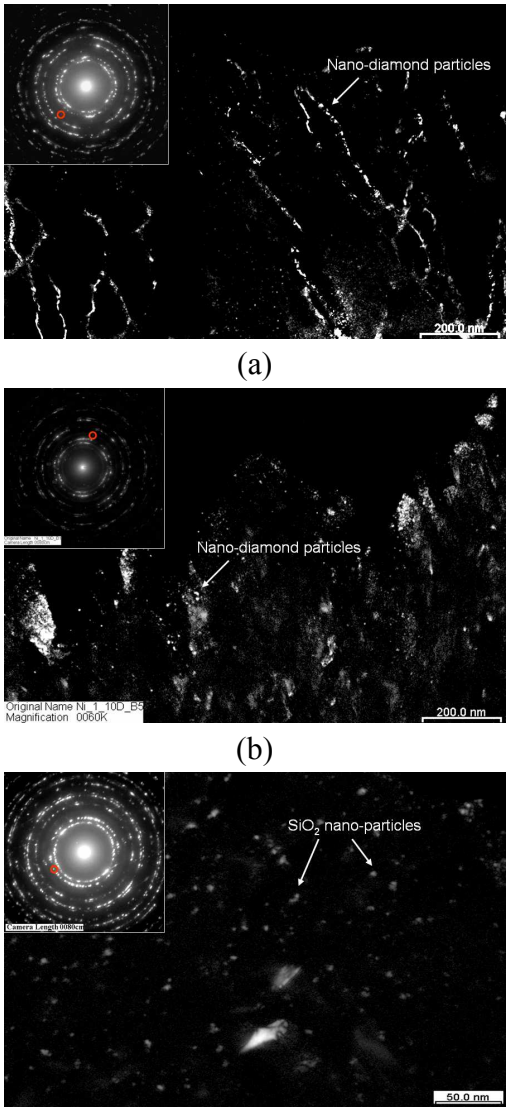

Fig. 9. Dark field TEM images of electroplated (a) Ni-diamond nanocomposite (average diameter 350 nm, 2 g/L, 0.47% v/v), (b) Ni-diamond nanocomposite (average diameter 50 nm, 2 g/L, 1.87% v/v), and (c) Ni-SiO2 nanocomposite (average diameter 80 nm, 0.036 g/L).

Fig. 9 shows the dark field TEM images of nano-diamond particles and nano-SiO_2 particles distribute in the Ni matrix. In this observation scale of Ni-diamond nanocomposite, we found that nano-diamond particles have different distribution in Ni matrix with different adding particle size in the plating bath. In Fig. 9a, the nano-diamond particles distribute in the grain boundary regions of the Ni matrix as the adding particle size is 350 nm in average diameter inside plating bath. However, with size the reduction of the adding diamond particles from 350 nm to 50 nm in plating bath, the distribution of nano-diamond particles migrate from grain boundary regions into Ni grains

as shown in Fig. 9b. Similarly, the intra-distribution of nano-particles in Ni grains is also observed on Ni-SiO_2 nanocomposite in Fig. 9c. As carried before, the CTE value of Ni-based nanocomposite comparing to Ni matrix would decrease due to the size reduction of adding diamond and different particle type like SiO_2. From the TEM analysis of crystalline texture in Fig. 9b and 9c, it is observed that the common point between diamond and SiO_2 nano-particles is intra-grain distribution. This intra-grain distribution of nano-particles will cause the residual tensile stresses inside Ni grains which decrease the CTE value of Ni-based nanocomposite. Oppositely, as shown in TEM analysis of Fig. 9a the inter-grain distribution of nano-particles will cause the residual compressive stresses inside Ni grains which increase the CTE value of Ni-based nanocomposite.

4. Conclusions

This paper reveals several new composite effects on the material property modification, especially on CTE, based on the incorporation of diamond or SiO_2 nano-particles into Ni matrix by low-temperature electrodeposited process. Through a simple composite-plating process, material properties can be modified easily in the expected way. In addition, electrodeposited Ni-based nanocomposites are compatibility with MEMS and CMOS fabrication technologies via a one-step, selective on-chip deposition process at low temperatures. These Ni-based nanocomposites are not only attractive for performance modification on CTE and Young's modulus but also may provide an alternative direction in the development of other MEMS devices using nanocomposites.

Reference

[1] W. Ehrfeld, F. Götze, D. Münchmeyer, W. Schelb, and D. Schmidt, "LIGA process: Sensor construction techniques via X-ray lithography," in *Technical Digest, IEEE Solid-State Sensor and Actuator Workshop*, Hilton Head, SC, pp. 1–4, 1988.

[2] S. Furukawa, S. Roy, H. Miyajima, Y. Uenishi, and M. Mehregany, "Nickel surface micromachning," in *Proc. IEEE Microstructures and Microfabricated Systems,* San Francisco, CA, pp. 38–46, 1994.

[3] Q. Shi, S.C. Chang, M.W. Putty, and D.B. Hicks, "Characterization of electroformed nickel microstructures," in *Proc. SPIE*, vol. 2639, pp. 191–199, 1995.

[4] P.M. Zavracky, S. Majumber, and E. McGruer, "Micromechanical switches fabricated using nickel surface micromachining," *J. Microelectromech. Syst.*, vol. 6, no. 1, pp. 3–9, 1997.

[5] C.P. Hsu, W.C. Tai, and W. Hsu, "Design and analysis of an electrothermally driven long-stretch micro drive with cascaded structure," in *Proc. ASME International Mechanical Engineering Congress & Exposition*, New Orleans, Louisiana, 2002.

[6] K. Kataoka, S. Kawamura, T. Itoh, K. Ishikawa, H. Honma, and T. Suga, "Electroplating Ni micro-cantilevers for low contact-force IC probing, *Sens. Actuators A*, vol. 103, pp. 116–121, 2003.

[7] A.F. Zimmerman, G. Palumbo, K.T. Aust, and U. Erb, "Mechanical properties of nickel silicon carbide nanocomposites," *Mater. Sci. Eng. A*, vol. 328, pp. 137–146, 2002.

[8] J. Steinbach and H. Ferkel, "Nanostructured Ni-Al_2O_3 films prepared by DC and pulsed DC

electroplating," *Scripta Mater.*, vol. 44, pp. 1813–1816, 2001.

[9] X. Li and Z. Li, "Nano-sized Si_3N_4 reinforced NiFe nanocomposites by electroplating," *Mater. Sci. Eng. A*, vol. 358, pp. 107–113, 2003.

[10] K.S. Teh, Y.T. Cheng, and L. Lin, "MEMS fabrication based on nickel-nanocomposite: film deposition and characterization," *J. Micromech. Microeng.*, vol. 15, pp. 2205–2215, 2005.

[11] Y.W. Huang, T.Y. Chao, C.C. Chen, and Y.T. Cheng, "Power consumption reduction scheme of magnetic microactuation using electroplated Cu–Ni nanocomposite," *Appl. Phys. Lett.*, vol. 90, 244105 , 2007.

[12] L.N. Tsai, G.R. Shen, Y.T. Cheng, and W. Hsu, "Performance improvement of an electrothermal microactuator fabricated using Ni-diamond nanocomposite," *J. Microelectromech. Syst.*, vol. 15, pp. 149–158, 2006.

[13] D. Schneider and M.D. Tucker, "Non-destructive characterization and evaluation of thin films by laser-induced ultrasonic surface waves," *Thin Solid Films*, vol. 290-291, pp. 305–311, 1996.

[14] A.J. Owen and I. Koller, "A note on the Young's modulus of isotropic two-component materials," *Polymer*, vol. 37, pp. 527–530, 1996

[15] M.T. Kim, "Influence of substrates on the elastic reaction of films for the microindentation tests," *Thin Solid Films*, vol. 283, pp. 12–16, 1996.

[16] A.A. Fahmy and A.N. Ragai, "Thermal-expansion behavior of two-phase solids," *J. Appl. Phys.*, vol. 41, pp.5108–5111, 1970.

[17] S. Lemieus, S. Elomari, J.A. Nemes, and M.D. Skibo, "Thermal expansion of isotropic Duralcan metal–matrix composites," *J. Mater. Sci.*, vol. 33, pp. 4381–4387, 1998

[18] C.L. Hsieh and W.H. Tuan, "Elastic and thermal expansion behavior of two-phase composites," *Mater. Sci. Eng. A*, vol. 425, pp. 349–360, 2006.

[19] D.D.L. Chung, "Materials for thermal conduction," *Appl. Therm. Eng.*, vol. 21, pp. 1593–1605, 2001.

[20] K.Tanaka and Y. Akiniwa, "Diffraction measurements of residual macrostress and microstress using X-rays, synchrotron and neutrons," *JSME Int. J. Ser. A*, vol. 47, pp. 252-263, 2004.

[21] W. Fang and C.Y. Lo, "On the thermal expansion coefficients of thin films," *Sensor. Actuat. A*, vol. 84, pp.310-314, 2000.

將在 IEEE Transducers 2009 研討會發表之論文

時間：2009 年 6 月 21 日至 6 月 25 日
地點：美國 科羅拉多州 丹佛
June 21-25, 2009 - Denver, Colorado, USA

報告人：交通大學機械系博士生 黃家聖
NSC 97-2221-E-020-MY3
註：此報告繳交時間為五月底，故尚無法附上心得報告

YOUNG'S MODULUS AND FATIGUE LIFETIME IMPROVEMENTS BY DIAMOND SIZE EFFECT ON ELECTROPLATED NI-DIAMOND NANOCOMPOSITE

C.S. Huang[1], Y.T. Cheng[2], C.J. Yeh[1], H.K. Liu[3], and W. Hsu[1]*
[1]Department of Mechanical Engineering, National Chiao Tung University, Taiwan
[2]Department of Electronics Engineering, National Chiao Tung University, Taiwan
[3]Department of Mechanical and Computer Aided Engineering, Feng Chia University, Taiwan

ABSTRACT

Fatigue and Young's modulus characterizations have been investigated using the bending-test method on microsized cantilever-beam specimens made of electroplated Ni and Ni-diamond nanocomposites with different particle sizes (i.e. 350nm and 50nm in diameter). The experimental results show that electroplated Ni-diamond nanocomposite has slightly smaller fatigue strength than that of pure electroplated Ni due to the ductility reduction resulted by the nano-diamond particles. However, once the incorporated particle size of nano-diamond is reduced from 350nm to 50nm, it has been found that the electroplated Ni-diamond nanocomposite can have higher Young's modulus (13.6% enhancement, i.e. 178GPa) and comparable fatigue strength (~2.4GPa) with that of pure electroplated Ni.

KEYWORDS

Bending-test, Thin film, Fatigue, Young's modulus, Nanocomposite, MEMS

INTRODUCTION

Nanotechnology has advanced the electro-deposition technique for high performance microelectro-mechanical systems (MEMS) fabrication in terms of material property enhancement by composite effect [1-5]. Previous reports have shown that electroplated Ni-diamond nanocomposite in comparison with pure electroplated Ni can have modified Young's modulus, hardness, and coefficient of thermal expansion (CTE). Tsai *et al.* [4] found that electro-thermal microactuator made of Ni-diamond nanocomposite can have 73% power consumption saving in comparison with that made of pure Ni for the same output displacement via the CTE enlargement of structural material. In addition, more than 67% ultimate elongation can be achieved. Lee *et al.* [5] demonstrated μ-resonator made of Ni-diamond

nanocomposite can have higher resonance frequency than the pure Ni one by Young's modulus improvement of structural material, and can make itself practical for electro-mechanical signal processing application to RF system. Thus, Ni-diamond nanocomposite has been thought as a potential structure material for further application in MEMS devices.

Nevertheless, up to now, related fatigue behavior of the electroplated Ni-diamond nanocomposite and long term reliability of the composite devices have not been well studied and examined. Since the investigation is essential for the design and fabrication of potential MEMS or components which are made of the nanocomposite and subjected to cyclic load. In this paper, the fatigue and Young's modulus of electroplated Ni and Ni-diamond nanocomposites will be thoroughly characterized by employing the bending-test method. The Ni-Diamond nanocomposites incorporated with different particle sizes (i.e. 350nm and 50nm in diameter) have also been investigated

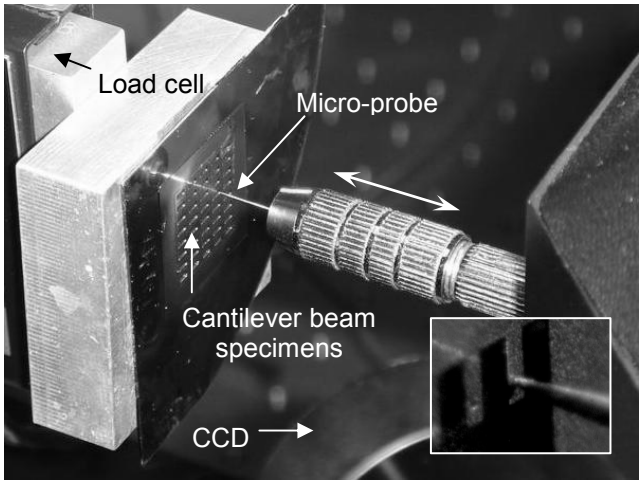

Figure 1: Set-up of fatigue test for cantilever-beam specimens.

DESIGN AND FABRICATION

Fig. 1 shows the set-up of fatigue test employing the bending method that microsized cantilever-beam specimen is tested in a displacement-control mode. A tungsten micro-probe controlled by test machine cyclically, 20Hz, applies a sinusoidal load on the free end of cantilever-beam specimen with a certain vertical displacement [6]. Through the charge-coupled device (CCD) system, the micro-probe can accurately be placed on the right load-position of cantilever-beam specimen. The loading force is measured by a load cell under the tested sample. In this fatigue test machine, the resolutions of load cell and displacement actuation can be controlled at 0.1mN and 0.1μm, respectively.

As shown in Fig. 2, the microsized cantilever-beam specimens are fabricated on a silicon substrate. Initially, 200Å thick Ti adhesion layer and 1000Å thick Cu seed layer are sputtered respectively onto a silicon wafer. After that, a 20μm thick AZP-4620 photoresister (PR) is coated and patterned to form plating molds (Fig. 2(a)). Subsequently, electroplated Ni-based material is deposited to form microsized cantilever-beam specimens (Fig. 2(b)). For the composite plating of Ni-diamond nanocomposites, two kinds of nano-diamond powders, 350nm and 50nm in diameter, are added respectively into sulfuric-based electroplating Ni baths for the fabrication of Ni-diamond nanocomposite beams. The concentrations of

nano- diamond particles in plating baths are all kept at 2g/L. At final, the as-fabricated cantilever-beam specimens are released after stripping the plating molds by acetone solution and the silicon underneath the beams is removed by KOH solution (Fig. 2(c)). According to the elemental analyzer measurement of the synthesized Ni-diamond nanocomposites with different particle sizes (i.e. 350nm and 50nm in diameter), the diamond contents of both nanocomposite specimens are very similar i.e. 0.15±0.01% in weight fraction.

Fig. 3 shows the SEM pictures of as-fabricated specimens made of electroplated Ni and Ni-diamond nanocomposite for the fatigue test, respectively. A contact hole is introduced in the specimen design as the load-position to fix the micro-probe with specimen for preventing the probe-tip from gliding along the beam during the test [7]. The contact hole, 15μm in diameter, is located on the center line of cantilever beam with 130μm from the beam-root and 50μm from the free-end. The designed width and thickness of the microsized cantilever-beam specimen are fixed at 50μm and 15μm, respectively.

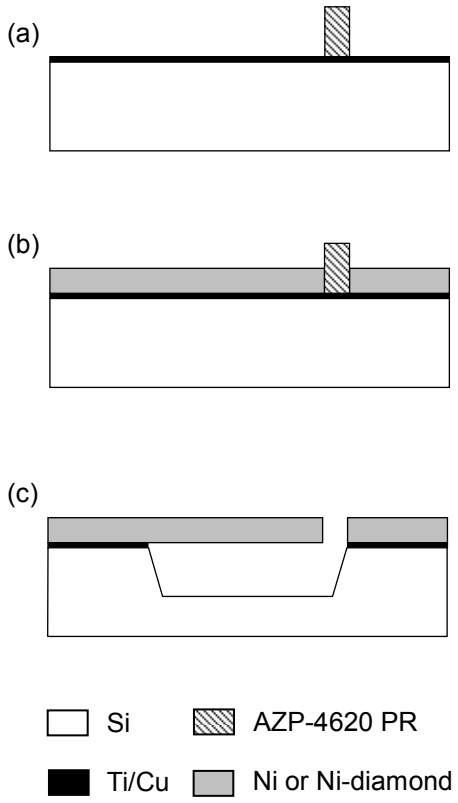

Figure 2: Fabrication process of cantilever-beam specimen.

RESULTS AND DISCUSSIONS

Static Bending Test

A static bending test is first performed on cantilever-beam specimens to determine the maximum displacement (δ_{max}) as fatigue test condition. The cantilever-beam specimen is gradually deflected by placing the tungsten micro-probe to the contact hole, and the loading force applied by the probe to the beam is measured by a load cell connected to the computer. Thus, the loading force versus corresponding displacement can be recorded as shown in Fig. 4. From the measured force-displacement (F-δ) curve, the maximum loading range is determined by the proportional limit of the curves. Under this range, the force is

proportional to the displacement.

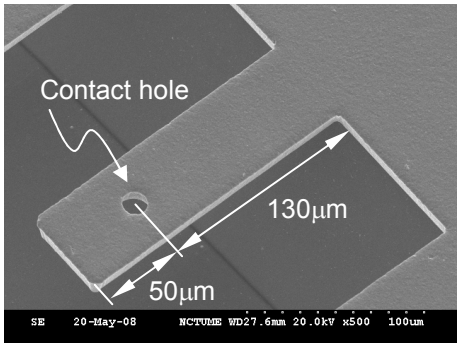

(a)

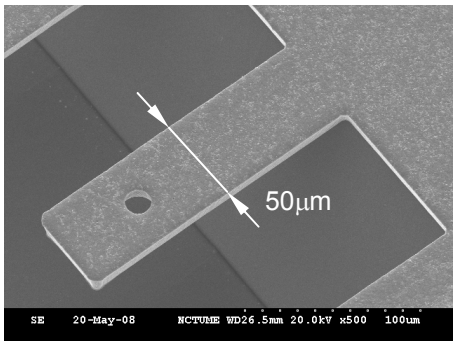

(b)

Figure 3: SEM pictures of fabricated cantilever-beam specimens: (a) Ni; (b) Ni-diamond (350nm in diameter).

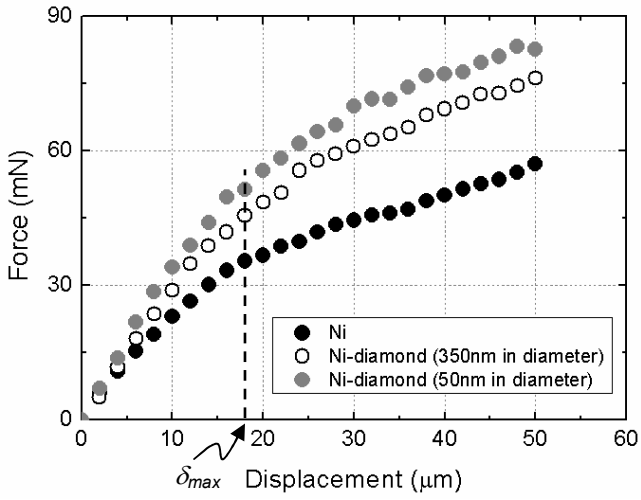

Figure 4: F-δ curves of microsized cantilever-beam specimens from static bending tests.

Young's Modulus Measurement

In Fig. 4, the *F-δ* curves also indicate the incorporation of nano-diamonds in Ni can enhance the stiffness (i.e. the ratio of force to displacement) of specimen. Using this experimental stiffness data and considering actual boundary conditions like quarter-plane and undercut which usually occur in wet-etching process [8], the Young's moduli of electroplated Ni and Ni-diamond nanocomposites can be estimated by finite element analysis (FEA) software of ANSYS. Once the analytical stiffness value of beam model from FEA is

matched with the experimental one from F-δ curves of Fig. 4, the corresponding Young's modulus can be obtained as shown in Fig. 5, and the values are 156.9GPa, 165.9GPa, and 178.2GPa for the electroplated Ni and Ni-diamond nanocomposites which are incorporated with the diamond nano-powders with the average particle diameter of 350nm and 50nm, respectively.

To further examine the derived Young's modulus values from F-δ data, the following measurement equipments of nanoindenter and laser Doppler vibrometer (LDV) are also performed. Using the nanoindenter measurement [3, 9], the Young's modulus is characterized directly from the electroplated film. The indentation depth is set as 1/10 film thickness, and the measured value is the average over twenty test points. The measured Young's moduli of Ni and Ni-diamond nanocomposite by means of indentation test are found to be 156.7±5GPa, 164.0±5GPa, and 178.0±5GPa for the electroplated Ni and Ni-diamond nanocomposites with the average particle diameter of 350nm and 50nm, respectively. Meanwhile, the Young's modulus is characterized based on the resonant frequency of electroplated beam measured by LDV [4, 10]. Once the analytical value of resonant frequency of beam model from FEA is matched with the experimental one from LDV, the corresponding Young's moduli can be obtained as 158.1±2GPa, 163.3±2GPa, and 178.2±2GPa for the electroplated Ni and Ni-diamond nanocomposites with the average particle diameter of 350nm and 50nm, respectively.

According to the above measurement results, the derived Young's modulus values from nanoindenter and LDV methods well agree with the one estimated by F-δ data. It is also noted that Ni-diamond nanocomposites with 350nm and 50nm in diameter can have around 4.6% and 13.6% Young's modulus enhancement than that of pure electroplated Ni, respectively.

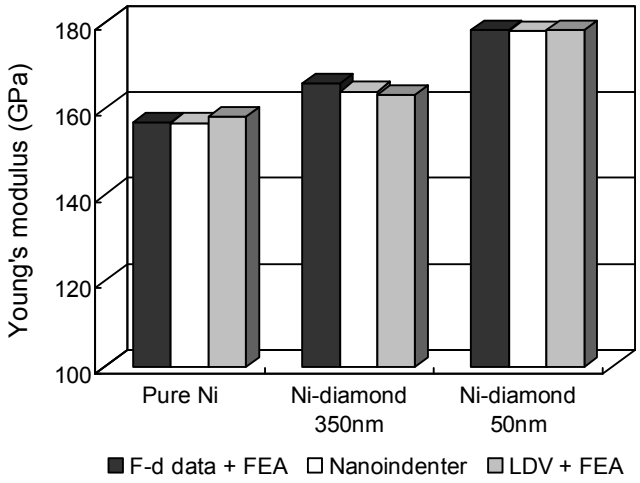

Figure 5: Young's modulus values of the electroplated Ni and Ni-diamond nanocomposites measured by F-d data + FEA, nanoindenter, and LDV + FEA methods.

Fatigue Lifetime Test

Fatigue lifetime test of the beams made of electroplated Ni and Ni-diamond composites are performed using the same micro-probe controlled by the test machine to cyclically apply a sinusoidal displacement on the free-end of cantilever beam with a frequency of 20Hz. Fatigue lifetime is obtained from different cyclic displacement loadings which are below δ_{max} for each fatigue test condition. The results of fatigue lifetime

test are shown in Fig. 6 as *S-N* curves. The value of stress amplitude in Fig. 6 is evaluated by FEA based on the conditions of sample and loading. The analysis shows that the maximum stress happens at the root-corner of cantilever-beam specimen during the cyclic displacement loading. Besides, in Fig. 6, each data point is determined while the specimen is broken and the applied load to the specimen for a displacement is diminutive simultaneously.

In general, fatigue strength is defined as the loaded stress for a specimen without having failure after 10^6 cycles [11]. From this definition, the fatigue strengths of electroplated Ni and Ni-diamond nanocomposites (i.e. 350nm and 50nm in diameter) are obtained as 2.41GPa, 2.18GPa, and 2.40GPa in Fig. 6, respectively. It can be found that the fatigue strength of Ni-diamond nanocomposite can have 10% increase with the reduction of nano-diamond particle size from 350nm to 50nm, and the fatigue lifetime of Ni-diamond nanocomposite with the average particle diameter of 50nm would be the same as that of pure electroplated Ni in the low loading stress regime.

The fatigue test results also show that electroplated Ni-diamond nanocomposites have smaller fatigue strength than that of pure electroplated Ni in large stress regime. It can be explained by the ductility reduction due to nano-diamond incorporation. Nevertheless, with the decrease of incorporated diamond size, the fatigue strength of the nanocomposite can be as strong as the Ni, especially pronounced at low stress cycling. This fatigue lifetime improvement can be attributed to the particle size effect [12]. Under the same weight fraction, small diamond size means more diamond particles complicate the composite grain boundary system which will hinder dislocation motion and prevent crack growth.

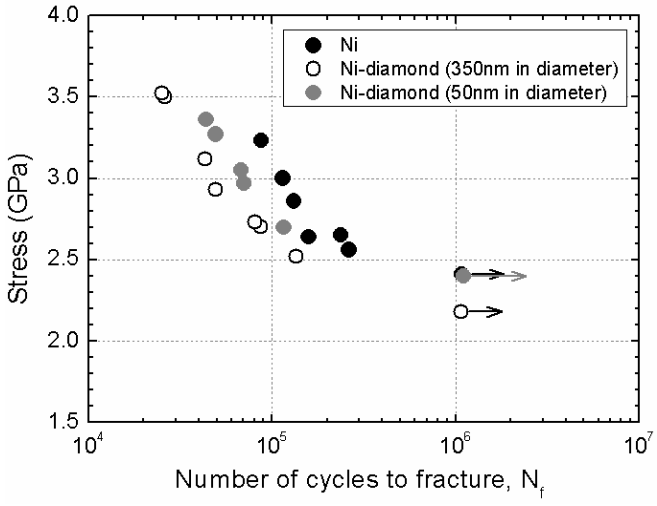

Figure 6: S-N curves of microsized cantilever-beam specimens from fatigue lifetime tests.

CONCLUSIONS

Characterizations of electroplated Ni and Ni-diamond nanocomposite including Young's modulus, fatigue lifetime, and fatigue strength, have been investigated by bending-test method using microsized cantilever-beam specimens. Due to the nano-diamond incorporation in the electroplated Ni matrix, the Young's modulus reinforcement of nanocomposite can be realized especially for small particle size. Furthermore, with the incorporation of small diamond size, the fatigue strength of the nanocomposite can be as strong as the Ni, especially pronounced at low stress cycling. Taking advantages of similar fatigue

strength as pure Ni, low electroplating temperature (~50 °C), and MEMS/CMOS compatible process, the electroplated Ni-diamond nanocomposite with enhanced Young's modulus is expected as an appropriate material for high frequency and actuating components of MEMS devices.

ACKNOWLEDGEMENTS

This work is supported by the National Science Council of Taiwan under Grant NSC 97-2221-E-009-020-MY3

REFERENCES

[1] K.S. Teh, Y.T. Cheng, L. Lin, "MEMS fabrication based on nickel-nanocomposite: film deposition and characterization", *J. Micromech. Microeng.*, vol. 15, pp. 2205-2215, 2005.

[2] Y.W. Huang, T.Y.Chao, C.C. Chen, Y.T. Cheng, "Power consumption reduction scheme of magnetic microactuation using electroplated Cu-Ni nano- composite", *Appl. Phys. Lett.*, vol. 90, pp. 244-105, 2007.

[3] C.S. Huang, Y.T. Cheng, J. Chung, W. Hsu, "Investigation of Ni-based thermal bimaterial structure for sensor and actuator application", *Sensor. Actuat. A*, vol. 149, pp. 298-304, 2009.

[4] L.N. Tsai, G.R. Shen, Y.T. Cheng, W. Hsu, "Performance improvement of an electrothermal microactuator fabricated using Ni-diamond nano- composite", *J. Microelectromech. Syst.*, vol. 15, pp. 149-158, 2006.

[5] Y.C. Lee, L.N. Tsai, Y.T. Cheng, W. Hsu, "Performance enhancement of comb drive actuators utilizing electroplated nickel-diamond nanocomposite", in: *Proceeding of APCOT*, Singapore, 2006.

[6] H.K. Liu, B.J. Lee, P.P. Liu, "Low cycle fatigue of single crystal silicon thin films", *Sensor. Actuat. A*, vol. 140, pp. 257-265, 2007.

[7] C.J. Wilson, A. Ormeggi, M. Narbutovskih, "Fracture testing of silicon microcantilever beams", *J. Appl. Phys.*, vol. 79, pp. 2386-2393, 1996.

[8] C. Hsu, C. Tsou, W. Fang, "Measuring thin film elastic modulus using a micromachined cantilever bending test by nanoindenter", *J. Micro/Nanolith. MEMS MOEMS*, vol. 6, pp. 033011, 2007.

[9] A.C. Fischer-Cripps, *Nanoindentation*, Springer, New York, 1st ed., pp. 27-30, 2002.

[10] L. Kiesewetter, J.M. Zhang, D. Houdeau, A. Steckenborn, "Determination of Young's moduli of micromechanical thin films using the resonance method", *Sensor. Actuat. A*, vol. 35, pp. 153-159, 1992.

[11] J.E. Shigley, C.R. Mischke, R.G. Budynas, *Mechanical Engineering Design*, Mc Graw Hill, New York, 7th ed., pp. 313-315, 2003.

[12] N. Chawla, C. Andres, J.W. Jones, J.E. Allison, "Effect of SiC volume fraction and particle size on the fatigue resistance of a 2080 Al/SiC_p composite", *Metall. Mater. Trans. A*, vol. 29, pp. 2843-2854, 1998.